THE JOURNAL OF PHYSICAL CHEMISTRY C

Article

pubs.acs.org/JPCC

Interplay between Electronic Properties and Interatomic Spacing in Artificial Gold Chains on NiAl(110)

N. Nilius,[§] T. M. Wallis,[†] M. Persson,[‡] and W. Ho*

Department of Physics and Astronomy and Department of Chemistry, University of California, Irvine, California 92697-4575, United States

ABSTRACT: Monatomic Au chains with 2.89 and 4.08 Å interatomic spacing were constructed on a NiAl(110) surface, using atom manipulation techniques with a scanning tunneling microscope. Differential conductance spectra taken on the two chains revealed a series of unoccupied quantum well states that exhibit the parabolic dispersion of a free-electron-like band. The effective electron mass of the band, a measure of the coupling strength between the Au atomic orbitals, was found to be two times smaller in the compact (0.5 m_e) than that in the loosely packed chain (0.94 m_e). Moreover, the band onset shifted toward the Fermi level (1.5 versus 0.75 eV) with decreasing distance between the Au atoms. The interrelation between geometric and electronic properties of the two chains was analyzed with density functional theory calculations and tight binding modeling. In the compact chain, the large orbital overlap results in a relatively steep parabolic electron band with strong Au 6sp character. The band flattens out as the interatomic distance increases in the more open Au chain. In both cases, the NiAl support leads to a renormalization of the band properties that arises from a hybridization between the Au 6sp atomic states and the NiAl bulk bands.

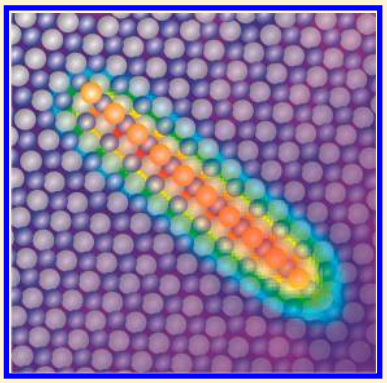

1. INTRODUCTION

Structural and electronic properties of matter are tightly interrelated. The mutual interactions are particularly strong in spatially confined, low-dimensional systems, the physical and chemical properties of which are governed by electron quantization effects and an enhanced influence of the surface. In fact, completely new physical phenomena may occur in nanosystems, for instance, the crossover from Fermi liquid to Luttinger-type behavior of the conduction electrons,[1] renormalized transport effects for heat and carriers,[2,3] and unusual magnetic properties.[4,5] The underlying physics is still not well-understood and therefore in the focus of active research.

Linear chains of metal atoms represent an ideal model system to study the interplay between structure and electronic properties as the coupling is restricted to one spatial dimension.[6] High-quality and essentially defect-free atom chains can be fabricated nowadays by various techniques, for example, atom deposition on suitable template surfaces,[7] self-assembly processes of metal−semiconductor adsystems,[8,9] and metal−organic growth.[10] Alternatively, manipulation techniques with the STM can be employed to build nanostructures on an atom-by-atom scheme. By exploiting this fascinating capability, quantum corrals,[11] molecular cascades for simple logical operations,[12] as well as atomic chains and clusters with pronounced electron quantization effects have been assembled.[13−16] The electronic characteristics of these nanostructures have been explored by angle-resolved photoelectron spectroscopy, four-probe conductance measurements, and more recently by STM-based state-density spectroscopy. The results have been corroborated by electronic structure and nonequilibrium transport calculations performed for a variety of nanostructures with different geometry, elemental composition, magnetic structure, and chemical environment.[17−19]

Typical surface science approaches to fabricate monatomic chains have the disadvantage that relevant chain parameters, such as the interatomic distance, are fixed by the substrate geometry. As a result, the chain properties are inseparably connected to the ones of the support, and the intrinsic properties of the chains can often not be determined. In an idealized computer experiment, on the other hand, the atom−atom separation and the vertical distance from the support can be freely adjusted, allowing for a disentanglement of intrinsic and support-induced properties of the adchains. Experimentally, the problem has been addressed by electronically decoupling the chains from the support, for instance, by growing them on chemically inert and weakly interacting surfaces. Moreover, different lattice parameters could be realized by fabricating the nanostructures on one and the same substrate, however along different crystallographic directions. Whereas the first approach has already been followed in a couple of examples, such as on semiconductors, oxides, and halide surfaces,[20,21] the second one has not been explored so far.

In this paper, we report a combined STM and DFT study on monatomic Au chains that were assembled along two crystallographic directions of a NiAl(110) support and have

Special Issue: John C. Hemminger Festschrift

Received: February 26, 2014
Revised: April 12, 2014

   dx.doi.org/10.1021/jp502036q | J. Phys. Chem. C XXXX, XXX, XXX−XXX

therefore different interatomic spacing. The chains display discrete resonance states, the nature and origin of which were analyzed with DFT and tight binding (TB) calculations. The different atom−atom distances give rise to a different degree of hybridization between the Au adatom orbitals in the chains that in turn alters the dispersion of the resulting electronic bands.

2. EXPERIMENT AND THEORY

The experiments have been performed in an ultrahigh vacuum STM operating at 12 K.[22] The NiAl(110) surface was prepared by cycles of Ne^+ sputtering and annealing to 1300 K. The alloy surface consists of alternating rows of Al and Ni atoms running along the [001] direction. Due to a slight outward relaxation of the Al atoms with respect to Ni, the Al rows appear as protruding lines in topographic STM images (Figure 1A). Gold

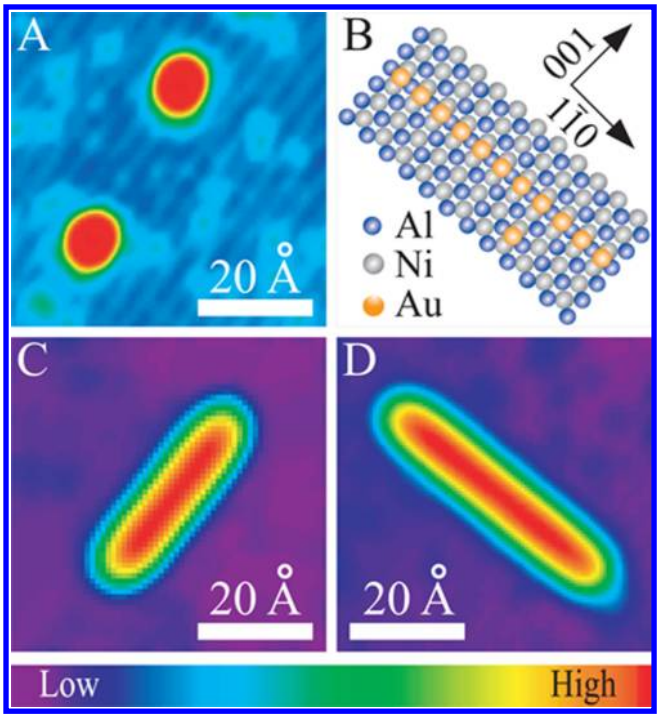

Figure 1. (A) STM topographic image of two Au atoms on NiAl(110). The contrast is enhanced to visualize the row-trough structure of the NiAl surface. (B) Structure model of a Au adatom and a [1$\bar{1}$0]-oriented Au_{11} chain on NiAl(110). STM images of a Au_{11} chain constructed (C) along the [001] and (D) along the [1$\bar{1}$0] directions of NiAl(110). All images are 55 Å × 55 Å in size and were taken at V_{sample} = 2.0 V and I = 1.0 nA.

atoms were evaporated from a crucible and deposited at 12 K onto the surface to suppress diffusion. The individual adatoms, imaged as round protrusions, preferentially adsorb on short Ni−Ni bridge sites (Figure 1B). The operation of the STM could be switched between an imaging and a manipulation mode by changing the tunneling resistance from the GΩ range to approximately 150 kΩ. In the manipulation regime, the Au atoms follow the trajectory of the tip (pulling mode) and can be assembled into linear nanostructures. The two-fold symmetry of the NiAl(110) promotes fabrication of Au chains with two different orientations. Whereas along the [001]-oriented Ni troughs the spacing of the chain atoms amounts to 2.89 Å, similar to the nearest-neighbor distance in bulk gold (2.88 Å), it increases to 4.08 Å in the perpendicular [1$\bar{1}$0] direction. STM topographic images of two Au_{11} chains assembled along the [001] and [1$\bar{1}$0] directions of NiAl are shown in Figure 1C and D.

Theoretical insight into the properties of the adchains was provided by DFT calculations, performed with the projector augmented wave method and the generalized gradient approximation, as implemented in the VASP code.[23,24] The Au chains were modeled as infinite succession of Au atoms sitting in Ni−Ni bridge sites of the NiAl(110) surface (see Figure 1B). The [001] and [1$\bar{1}$0] chains were placed on (1 × 4) and (6 × 1) supercells of a nine layer thick NiAl slab, being separated by 12 Å of vacuum from its replica in the vertical direction. Structural optimization was carried out for the Au atoms and the two outermost NiAl planes.[25] The role of direct and substrate-mediated interactions was determined by comparing the electronic properties of supported and free-standing Au chains with identical interatomic distance.[26] To make contact to scanning tunneling spectroscopy (STS), we have calculated the local density of states (LDOS) at the position of the tip apex, using the unoccupied Kohn−Sham states. The bias dependence of the tunneling barrier was accounted for by extending the sample wave functions into the vacuum. The respective decay parameter was deduced from the mean barrier height in the tip−sample region.[27]

3. RESULTS AND DISCUSSION

The electronic properties of the Au chains were investigated by STS, detecting the differential conductance (dI/dV) of the tip−sample junction with the lock-in technique. The dI/dV signal provides a measure of the sample LDOS at the position of the tip apex.[28] Conductance spectra of single Au atoms exhibit a pronounced dI/dV peak at +2.0 V above the Fermi level (E_F) that is absent in spectra of the bare NiAl surface (Figure 2A).

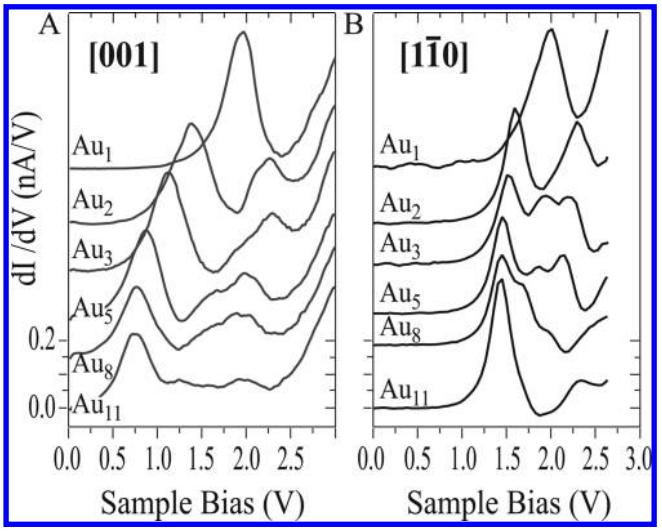

Figure 2. Conductance spectra taken in the center of differently long Au chains, assembled along (A) the [001] and (B) the [1$\bar{1}$0] directions of NiAl(110). The spectra were measured with V_{sample} = 2.5 V and I = 1 nA.

The peak reflects a resonance state that arises from hybridization of the Au 6sp orbital and NiAl electronic states and is located in a pseudo-gap of the NiAl bulk bands.[29] The assembly of two Au atoms into a [001]-oriented dimer causes the single-atom peak to split into two maxima at 1.4 and 2.2 V (Figure 2A). The splitting decreases to 0.6 V in the [1$\bar{1}$0]-oriented dimer that displays peaks at 1.65 and 2.25 V (Figure 2B). The

dx.doi.org/10.1021/jp502036q | J. Phys. Chem. C XXXX, XXX, XXX−XXX

reduced energy separation already reflects the larger interatomic distance in [1$\bar{1}$0] (4.08 Å) compared to that in [001] dimers (2.89 Å).[19] Three dI/dV peaks emerge in linear Au trimers, with the first one detected at 1.1 and 1.55 V for the [001] and [1$\bar{1}$0] configurations, respectively. The attachment of further atoms results in a continuous downshift of the leading dI/dV peak to finally 0.75 and 1.5 V in 11-atom [001] and [1$\bar{1}$0] chains, respectively. Simultaneously, new peaks develop at higher bias and shift toward E_F as the number of chain atoms increases. Due to their finite widths, adjacent dI/dV peaks overlap in the longer chains and finally merge into a continuous band.

To investigate the spatial variations in conductance, dI/dV spectral series have been taken along the axis of [001]- and [1$\bar{1}$0]-oriented Au_{11} chains (Figure 3A,B). Although the

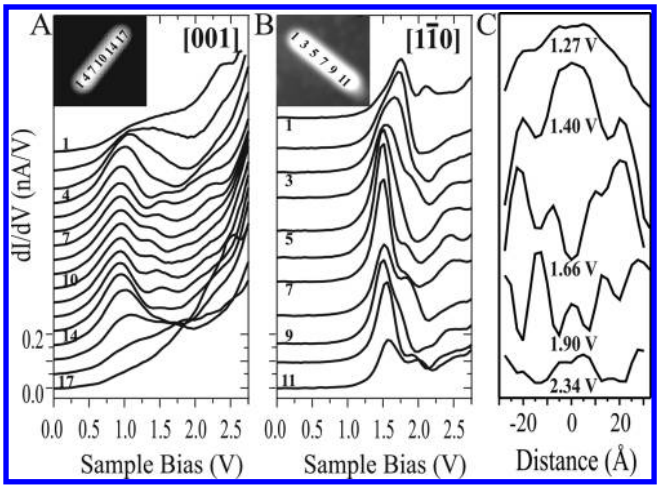

Figure 3. Conductance spectra taken along Au_{11} chains oriented along (A) the [001] and (B) the [1$\bar{1}$0] directions of NiAl(110). All spectra were acquired at V_{sample} = 2.5 V and I = 1 nA. Tip positions for spectroscopy are indicated in the insets. (C) Vertical cuts through the dI/dV series of panel (B) at the indicated bias voltages. The dI/dV oscillations along the chain axis have been fitted to a particle-in-a-box model to determine the energy position of eigenstates in the [1$\bar{1}$0] chain. See the text for details.

conductance is dominated by the low-energy peak at 0.75 and 1.5 V in the two chains, intensity oscillations along their axes become visible at higher bias. They can be visualized in cross sections through the dI/dV series at fixed bias voltages. Typical examples are shown for the [1$\bar{1}$0] Au_{11} chain in Figure 3C; the corresponding plots for the [001] chain can be found in the literature.[6] We note that dI/dV intensity oscillations are more pronounced along the [001]-oriented chains; however, the number of maxima and minima increases faster with bias for the [1$\bar{1}$0] conformer. The axial dI/dV intensity oscillations were analyzed with a "particle-in-a-box" model, describing the Au chains as 1D potential wells with infinite walls.[30] Wave functions in this 1D quantum system are sinusoidals $\sin(k_n x)$ with wave numbers $k_n = \pi n/L$ depending on quantum number n. The positions of eigenstates ε_n in the system were derived from fitting the dI/dV oscillations to a sum of squared wave functions weighted by a bias-dependent coefficient $c_n(V)$: $(dI/dV) \approx \sum_n c_n(V)|\sin(k_n x)|^2$. To account for the finite depth of the potential in the experiment, also the box length L was treated as an adjustable parameter. The obtained fit values for L were found to increase with the bias voltage, changing from 34 to 38 Å for [001] and from 50 to 58 Å for [1$\bar{1}$0] chains. Note that the geometrical chain lengths amount to 10 × 2.89 and 10 × 4.08 Å for the two chains, respectively, and are generally shorter than the fit values due to the diffusivity of the wave functions at the chain ends.

The fitting procedure revealed a Gaussian dependence of the coefficients c_n on the sample bias, with each maximum defining the energy position of an eigenstate ε_n (Figure 4C and D).[13] A

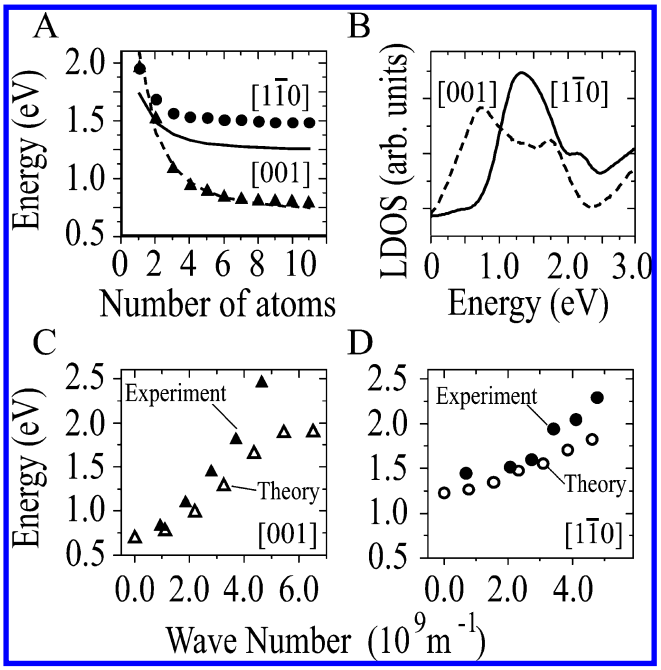

Figure 4. (A) Position of the lowest-energy dI/dV peak in [1$\bar{1}$0] and [001] Au chains as a function of the atom number in the chain. The symbols represent experimental data; the solid lines reflect the dependency derived from the calculated dispersion in infinite chains and an effective mass approximation. (B) Calculated LDOS for infinite [1$\bar{1}$0]- and [001]-oriented Au chains on NiAl(110). (C) Resonance states in a [001] Au_{11} chain as a function of the wavenumber k_n. Experimental and calculated points are depicted by filled and open symbols, respectively. The experimental points were obtained from fitting the bias-dependent dI/dV oscillations along the chain to a 1D particle-in-a-box model. The zone boundary is at k = 10.9 nm^{-1}. (D) As in (C) but for the [1$\bar{1}$0]-oriented Au_{11} chain. The zone boundary is at k = 7.7 nm^{-1}.

plot of the level energies ε_n versus the associated wavenumber k_n yields the dispersion of the electronic states, which was found to be parabolic in the two cases, $\varepsilon_n(k) = \varepsilon_0 + (\hbar^2/2m_{eff})k_n^2$. For the [001]-oriented Au_{11} chain, a band onset of ε_0 = 0.75 eV and an effective electron mass of m_{eff} = 0.5 m_e were determined, while the band parameters for the [1$\bar{1}$0] chain are ε_0 = 1.38 eV and m_{eff} = 0.94 m_e. We note that an effective mass similar to the free electron mass has not been observed for low-dimensional Au structures before, where m_{eff} is typically much smaller than m_e.[31−33]

To obtain insight into the nature of the resonance states, we have carried out DFT calculations on the geometric and electronic properties of supported [001] and [1$\bar{1}$0] Au chains. The calculations reveal the formation of unoccupied Au-derived resonance states that extend from 0.75 to 1.8 eV in the [001] chain but are confined to an energy range between 1.3 and 2.1 eV in the [1$\bar{1}$0] chain (Figure 4B). The dispersion of these states is obtained from LDOS versus wave number plots, as shown in Figure 4C and D. For both chain orientations, we find

dx.doi.org/10.1021/jp502036q | J. Phys. Chem. C XXXX, XXX, XXX−XXX

a nearly parabolic relationship in the first half of the Brillouin zone, corresponding to effective electron masses m_{eff} of 0.65 and 0.91 m_e for the [001] and [1$\bar{1}$0] chains, respectively. This agrees well with the values of 0.5 and 0.94 m_e, as derived from our conductance measurements. The change in the effective mass reflects the different degrees of hybridization between the Au orbitals in chains of different interatomic spacing. As expected, the interaction decreases with increasing lattice parameter a, a fact that becomes evident also in the reduced energy splitting $\Delta\varepsilon_{12}$ of the resonance doublet in [1$\bar{1}$0] (0.6 eV) and [001] dimers (0.9 eV). On the basis of these values, the effective electron mass around the Γ-point can be obtained with a nearest-neighbor TB model, using $m_{eff} = \hbar^2/(\Delta\varepsilon_{12}a^2)$. However, the derived masses, 1.0 and 0.75 m_e for [001] and [1$\bar{1}$0] chains, do not reproduce the experimental values. This discrepancy indicates that the interatomic coupling is not restricted to next-neighbor atoms, as required in the TB model, but extends over several atoms in the chain. We will discuss this point in more detail below. When inserting the DFT effective mass into our TB model, we are able to calculate the energy of the first resonance $\varepsilon_1(N)$ in the Au chains as a function of the atom number N, $\varepsilon_1(N) \approx \varepsilon_0 + (\hbar^2k_1^2/2m_{eff})$. Here, $k_1 = \pi/L$ denotes the wavenumber of the first state in a potential well with the length $L = (N+1)a$. Indeed, calculated and measured onset energies are in good agreement down to a single atom, as shown in Figure 4A.

To address the importance of long-range interactions between the chain atoms and the role of the metal substrate, we have calculated the electronic properties of free-standing Au chains that have the same interatomic spacing as the ones on the NiAl support. A comparison between free and supported chains is justified because the resonance states in the adfeatures develop from the Au 6s orbital of the free atoms upon adsorption. The evolution of the partial DOS with decreasing distance to the NiAl, Δd_{cs}, is illustrated for a [1$\bar{1}$0]-oriented chain in Figure 5. Whereas in the free chain the 6s band is mainly occupied (lower curve), it splits and broadens into two well-separated bands when approaching the surface. The states above E_F mix with the Au 6p manifold and form resonances with strong sp character (upper curve), the ones detected in the experiment. The width of the unoccupied sp band amounts to 1.04 eV in the free-standing [1$\bar{1}$0] chain (Figure 6), which is close to the TB value of 1.16 eV derived from the energy splitting ε_{12} in the [1$\bar{1}$0] dimer. In contrast, the 6s band of unsupported [001] chains has a substantially larger width in DFT (5.1 eV) than in the TB calculations (3.2 eV) (Figure 6). This difference demonstrates the long-range character of electronic interactions in the free-standing [001] chain, whereas only the next-neighbor atoms are involved in the [1$\bar{1}$0] chain.

The coupling between adatom resonances is however not only governed by direct orbital overlap but also substrate-mediated interactions play a crucial role. The hybridization with the NiAl electronic states leads to a delocalization of the 6s-like resonance states and lowers the spectral weight at the position of the initial 6s orbital. As a result, the interaction due to direct orbital overlap is attenuated, while indirect coupling via the substrate states gets enhanced. For the supported [001] dimer with its small binding length, the loss in direct coupling dominates, which renders the splitting of the resonance states three times smaller than that in the free dimer. Conversely, the enhanced substrate effect gives rise to a small effective mass and a large dispersion of resonance states in the supported [001] chain. In less compact [1$\bar{1}$0]-oriented dimers and chains, on the other hand, the attenuation of direct 6s overlap compensates for the promoting effect of the substrate, resulting in similar

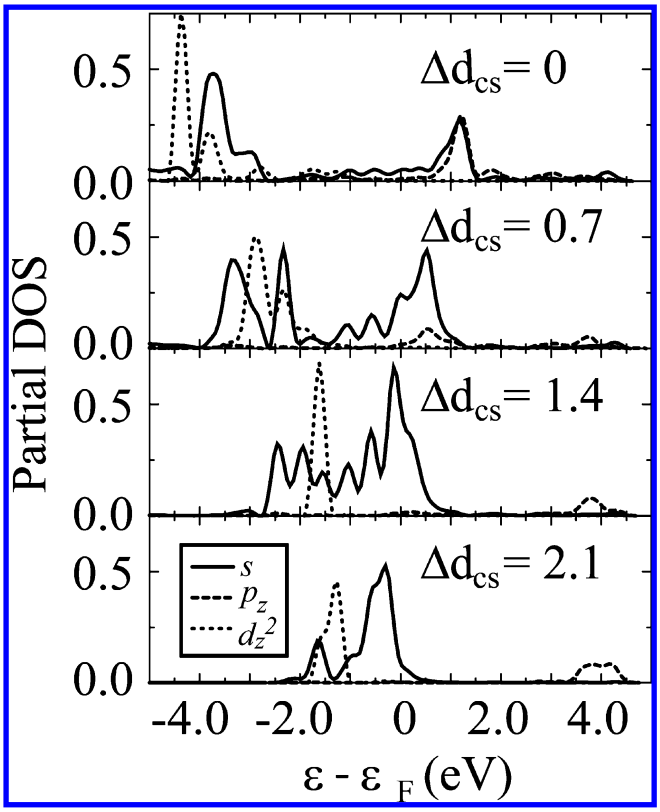

Figure 5. Partial wave decomposition of the Γ-point DOS of a Au atom in an infinite [1$\bar{1}$0] chain shown as a function of the vertical distance Δd_{cs} from the NiAl(110) surface. The s, p_z, and d_{z^2} character of the states is indicated by solid, dashed, and dotted lines, respectively.

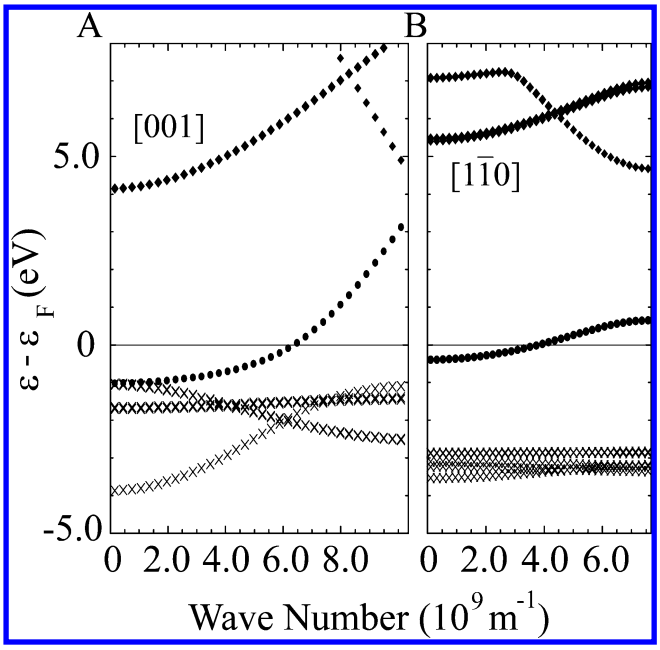

Figure 6. Calculated band structure of free-standing Au chains with the same lattice constants as those (A) in [001]- and (B) [1$\bar{1}$0]-oriented chains on NiAl(110). Bands with predominantly s, p, and d partial wave character are indicated by solid circles, diamonds, and crosses, respectively.

dx.doi.org/10.1021/jp502036q | J. Phys. Chem. C XXXX, XXX, XXX−XXX

effective masses and dispersion relations in the supported and nonsupported case. The specific electronic properties of chains with different lattice parameters can thus be rationalized only if both direct and substrate-mediated interactions are taken into account.

Finally, we want to stress that no changes in the regular atom spacing are observed for NiAl-supported Au chains in our STM images, which would be indicative of a Peierls distortion.[34−39] A likely reason is the strong adatom−substrate interaction that fixes the atom positions to the underlying lattice. Moreover, the resonance bands detected in the Au chains are unoccupied, and gap openings induced by a Peierls transition are thus ineffective in reducing the total energy of the system.

4. CONCLUSIONS

The capability of the STM to manipulate single Au atoms was exploited to construct well-defined monatomic chains on a NiAl(110) surface with two different lattice constants. Conductance measurements revealed the formation of free-electron-like bands in the two chains. The band in the compact chain displays a two times larger curvature and a lower onset energy than the band in the more open one. With the help of DFT calculations and TB modeling, the difference is ascribed to the varying impact of direct versus substrate-mediated coupling between the Au atomic orbitals. Whereas the direct orbital overlap scales directly with the spacing of the chain atoms, the indirect coupling leads to a certain attenuation of the orbital overlap especially at short distances. Our combined experimental and theoretical study provides insight into the fundamental interplay between geometric and electronic properties of quantum systems, providing information for the development of future nanoscale devices.

AUTHOR INFORMATION

Corresponding Author

*E-mail: wilsonho@uci.edu. Phone (949) 824-3492.

Present Addresses

[§]N.N.: Carl von Ossietzky University Oldenburg, Institute of Physics, D-26111 Oldenburg, Germany.

[†]T.M.W.: National Institute of Standards and Technology, Boulder, CO 80305, U.S.A.

[‡]M.P.: Surface Science Research Centre, University of Liverpool, Liverpool L69, U.K.

Notes

The authors declare no competing financial interest.

ACKNOWLEDGMENTS

Support of this research by the Chemical Sciences, Biosciences, and Geosciences Division, Office of Basic Energy Sciences, U.S. Department of Energy Grant No. DE-FG02-04ER15595 is gratefully acknowledged. N.N. thanks the Deutsche Forschungsgemeinschaft for a fellowship. M.P. is grateful for funding by the Swedish Research Council (VR) and for allocations of computer resources by SNAC.

REFERENCES

(1) Blumenstein, C.; Schäfer, J.; Mietke, S.; Meyer, S.; Dollinger, A.; Lochner, M.; Cui, X. Y.; Patthey, L.; Matzdorf, R.; Claessen, R. Atomically Controlled Quantum Chains Hosting a Tomonaga−Luttinger Liquid. *Nat. Phys.* **2011**, *7*, 776−780.

(2) Gao, S.; Yuan, Z. Emergence of Collective Plasmon Excitation in a Confined One-Dimensional Electron Gas. *Phys. Rev. B* **2005**, *72*, 121406(R).

(3) Krieg, U.; Brand, C.; Tegenkamp, C.; Pfnür, H. One-Dimensional Collective Excitations in Ag Atomic Wires Grown on Si(557). *J. Phys.: Condens. Matter* **2013**, *25*, 014013.

(4) Hirjibehedin, C. F.; Lutz, C. P.; Heinrich, A. J. Spin Coupling in Engineered Atomic Structures. *Science* **2006**, *312*, 1021−1024.

(5) Khajetoorians, A. A.; Wiebe, J.; Chilian, B.; Lounis, S.; Blügel, S.; Wiesendanger, R. Atom-by-Atom Engineering and Magnetometry of Tailored Nanomagnets. *Nat. Phys.* **2012**, *8*, 497−503.

(6) Nilius, N.; Wallis, T. M.; Ho, W. Development of One-Dimensional Band Structure in Artificial Gold Chains. *Science* **2002**, *297*, 1853−1856.

(7) Gambardella, P.; Blanc, M.; Brune, H.; Kuhnke, K.; Kern, K. One-Dimensional Metal Chains on Pt Vicinal Surfaces. *Phys. Rev. B* **2000**, *61*, 2254−2262.

(8) Crain, J. N.; McChesney, J. L.; Zheng, F.; Gallagher, M. C.; Snijders, P. C.; Bissen, M.; Gundelach, C.; Erwin, S. C.; Himpsel, F. J. Chains of Gold Atoms with Tailored Electronic States. *Phys. Rev. B* **2004**, *69*, 125401.

(9) Zandvliet, H. J. W.; van Houselt, A.; Poelsema, B. Self-Lacing Atom Chains. *J. Phys.: Condens. Matter* **2009**, *21*, 474207−474214.

(10) Grill, L.; Dyer, M.; Lafferentz, L.; Persson, M.; Peters, M. V.; Hecht, S. Nano-Architectures by Covalent Assembly of Molecular Building Blocks. *Nat. Nanotechnol.* **2007**, *2*, 687−691.

(11) Crommie, M. F.; Lutz, C. P.; Eigler, D. M. Imaging Standing Waves in a Two-Dimensional Electron Gas. *Nature* **1993**, *363*, 524−527.

(12) Heinrich, A. J.; Lutz, C. P.; Gupta, J. A.; Eigler, D. M. Molecule Cascades. *Science* **2002**, *298*, 1381−1387.

(13) Nilius, N.; Wallis, T. M.; Ho, W. Realization of a Particle-in-a-Box: Electron in an Atomic Pd Chain. *J. Phys. Chem. B* **2005**, *109*, 20657−20660.

(14) Fölsch, S.; Hyldgaard, P.; Koch, R.; Ploog, K. H. Quantum Confinement in Monatomic Cu Chains on Cu(111). *Phys. Rev. Lett.* **2004**, *92*, 056803.

(15) Lagoute, J.; Liu, X.; Fölsch, S. Link between Adatom Resonances and the Cu(111) Shockley Surface State. *Phys. Rev. Lett.* **2005**, *95*, 136801.

(16) Sperl, A.; Kröger, J.; Néel, N.; Jensen, H.; Berndt, R.; Franke, A.; Pehlke, E. Unoccupied States of Individual Silver Clusters and Chains on Ag(111). *Phys. Rev. B* **2008**, *77*, 085422.

(17) Gonzalez, C.; Ortega, J.; Flores, F. Metal−Insulator Transition in One-Dimensional In-Chains on Si(111). *New. J. Phys.* **2005**, *7*, 100.

(18) Mohn, F.; Repp, J.; Gross, L.; Meyer, G.; Dyer, M. S.; Persson, M. Reversible Bond Formation in a Gold-Atom−Organic-Molecule Complex As Molecular Switch. *Phys. Rev. Lett.* **2010**, *105*, 266102.

(19) Nilius, N.; Wallis, T. M.; Persson, M.; Ho, W. Distance Dependence of the Interaction between Single Atoms: Gold Dimers on NiAl(110). *Phys. Rev. Lett.* **2003**, *90*, 196103.

(20) Fölsch, S.; Yang, J.; Nacci, C.; Kanisawa, K. Atom-by-Atom Quantum State Control in Adatom Chains on a Semiconductor. *Phys. Rev. Lett.* **2009**, *103*, 096104.

(21) Nilius, N.; Ganduglia-Pirovano, V.; Brazdova, V.; Kulawik, M.; Sauer, J.; Freund, H.-J. Counting Electrons Transferred through a Thin Alumina Film into Au Chains. *Phys. Rev. Lett.* **2008**, *100*, 096802.

(22) Stipe, B. C.; Rezaei, M. A.; Ho, W. A Variable-Temperature Scanning Tunneling Microscope Capable of Single-Molecule Vibrational Spectroscopy. *Rev. Sci. Instrum.* **1999**, *70*, 137−143.

(23) (a) Kresse, G.; Hafner, J. Ab-Initio Molecular Dynamics for Liquid Metals. *Phys. Rev. B* **1993**, *47*, 558−561. (b) Kresse, G.; Furthmuller, J. Efficient Iterative Schemes for Ab-Initio Total-Energy Calculations Using a Plane-Wave Basis Set. *Phys. Rev. B* **1996**, *54*, 11169−11186.

(24) Perdew, J. P.; Chevary, J. A.; Vosko, S. H.; Jackson, K. A.; Pederson, M. R.; Singh, D. J.; Fiolhais, C. Atoms, Molecules, Solids, And Surfaces: Applications of the Generalized Gradient Approximation for Exchange and Correlation. *Phys. Rev. B* **1992**, *46*, 6671−6687.

(25) The largest adatom-induced relaxation is a 0.1 Å downward shift of the Ni atoms below the [001] chain. The Au−surface distance was determined to be 2.05 Å (1.95 Å) for the [001] ([1$\bar{1}$0]) chain.
(26) Persson, M. Computational Study of Electron States in Au Chains on NiAl(110). *Phys. Rev. B* **2004**, *70*, 205420.
(27) Lang, N. D. Spectroscopy of Single Atoms in the Scanning Tunneling Microscope. *Phys. Rev. B* **1986**, *34*, 5947−5951.
(28) Tersoff, J.; Hamann, D. R. Theory of the Scanning Tunneling Microscope. *Phys. Rev. B* **1985**, *31*, 805−813.
(29) Lui, S. C.; Kang, M. H.; Mele, E. J.; Plummer, E. W.; Zehner, D. M. Surface States on NiAl(110). *Phys. Rev. B* **1989**, *39*, 13149−13159.
(30) Kittel, C. *Introduction To Solid State Physics*; Wiley: New York, 1996.
(31) Altmann, K. N.; Crain, J. N.; Kirakosian, A.; Lin, J.-L.; Petrovykh, D. Y.; Himpsel, F. J. Electronic Structure of Atomic Chains on Vicinal Si(111)-Au. *Phys. Rev. B* **2001**, *64*, 035406.
(32) Mugarza, A.; Mascaraque, A.; Perez-Dieste, V.; Repain, V.; Rousset, S.; Garcia, F. J.; Ortega, J. E. Electron Confinement in Surface States on a Stepped Gold Surface Revealed by Angle-Resolved Photoemission. *Phys. Rev. Lett.* **2001**, *87*, 107601.
(33) Stiehler, C.; Pan, Y.; Schneider, W.-D.; Koskinen, P.; Häkkinen, H.; Nilius, N.; Freund, H.-J. Electron Quantization in Arbitrarily Shaped Gold Islands on MgO Thin Films. *Phys. Rev. B* **2013**, *88*, 115415/1−115415/8.
(34) van Houselt, A.; Gnielka, T.; de Brugh, J. M. J. A.; Oncel, N.; Kockmann, D.; Heid, R.; Bohnen, K. P.; Poelsema, B.; Zandvliet, H. J. W. Peierls Instability in Pt Chains on Ge(001). *Surf. Sci.* **2008**, *602*, 1731−1735.
(35) Hasegawa, S. J. Quasi-One-Dimensional Metals on Semiconductor Surfaces with Defects. *Condens. Matter* **2010**, *22*, 084026.
(36) Aulbach, J.; Schäfer, J.; Erwin, S. C.; Meyer, S.; Loho, C.; Settelein, J.; Claessen, R. Evidence for Long-Range Spin Order Instead of a Peierls Transition in Si(553)-Au Chains. *Phys. Rev. Lett.* **2013**, *111*, 137203.
(37) Sanchez-Portal, D.; Artacho, E.; Junquera, J.; Ordejon, P.; Garcia, A.; Soler, J. M. Stiff Monatomic Gold Wires with a Spinning Zigzag Geometry. *Phys. Rev. Lett.* **1999**, *83*, 3884−3887.
(38) De Maria, L.; Springborg, M. Electronic Structure and Dimerization of a Single Monatomic Gold Wire. *Chem. Phys. Lett.* **2000**, *323*, 293−299.
(39) Okamoto, M.; Takayanagi, K. Structure and Conductance of a Gold Atomic Chain. *Phys. Rev. B* **1999**, *60*, 7808−7811.